Nuclear Engineering and Technology 52 (2020) 206–210

Contents lists available at ScienceDirect

Nuclear Engineering and Technology

journal homepage: www.elsevier.com/locate/net

Original Article

Investigation on failure assessment method for nuclear graphite components

Yantao Gao, Derek K.L. Tsang*

Division of Nuclear Materials Science and Engineering, Shanghai Institute of Applied Physics, Chinese Academy of Sciences Jia Luo Road 2019, Jiading District, Shanghai, 201800, China

ARTICLE INFO

Article history:
Received 17 April 2019
Received in revised form
3 June 2019
Accepted 4 July 2019
Available online 4 July 2019

Keywords:
Molten salt reactor
Graphite
ASME
KTA3232

ABSTRACT

Super fine-grained graphite is a type of advanced nuclear graphite which was developed for Molten Salt Reactor (MSR). It is necessary to establish a failure assessment method used for nuclear graphite components in MSR. A modified assessment approach based on ASME BPVC-III-5_2017 is presented. The new approach takes a new parameter, KIC, into account and abandons the parameter, grain size, which is unrealistic for super fine-grained graphite as the computation is enormous if we use conventional methods. Three methodologies (KTA 3232, ASME, New approach) were also evaluated by theoretical prediction and experimental verification. The results indicated the new developed code can be used for design and failure assessment of super fine-graphite components and has more extensive applicability.

1. Introduction

Molten Slat Reactor (MSR) is considered as one of the Generation IV nuclear power systems due to its intrinsical characteristics [1]. In thorium molten salt reactor nuclear energy system (TMSR) in China, graphite is designed as a structural and neutron-moderator material. Super fine-grained graphite (such as T220 manufactured by Sinosteel AMC, NG-CT-50 manufactured by Fangda Carbon New Material Co., Ltd) is supposed to be used to prevent molten salt infiltration. As we know, nuclear graphite has inherent defects, such as crystal irregularities, pores and cracks. These defects can reduce the material strength and result in a large scatter in experimental material strength [2,3] data. The failure assessment of nuclear graphite components must take into account such variability in the strength data.

Probabilistic failure analysis is widely used to assess nuclear graphite components. In the 1970s, a German draft standard (KTA 3232 [4]) had been formed mentioned to perform probabilistic failure analysis for graphite components in early gas-cooled nuclear reactors. Many researchers [5–8] tried to predict the failure of a graphite component by Weibull aproach by using the estimates obtained by test results of small specimens. However, the results were always inconsistent with the experimental results. The reason could be attributed to incomplete consideration of the volume effect in brittle materials. Recently, M. P. Hindley [9] developed an approach for predicting failure in NBG-18 nuclear graphite components in a nuclear core design for Pebble Bed Modular Reactor. However, for super fine-grained graphite in TMSR, the average grain size is less than 20 μm and the fracture toughness (KIC) is relatively low (~0.8–1). The existing assessment methodology of nuclear graphite needs to be improved for the fine grained graphite.

To seek a methodology which is more suitable for the failure assessment for the fine nuclear graphite components. A modified assessment approach based on ASME BPVC-III-5_2017 [10] is presented in this paper. The new approach was compared with conventional approaches (KTA 3232 and ASME). And four point bending tests of Dog-Bone specimens and Brazilian disc splitting tests were implemented to validate the new developed approach.

2. Failure calculation methodology

In this paper, the requirement of the failure assessment methodology presented is to predict the probability of failure (POF) of a graphite component under a given stress state. The methodology employed is a modified volume normalized Weibull weakest link failure criterion. The total POF is the product of the POF of each link in this weakest link formulation.

* Corresponding author.
E-mail address: gaoyantao@sinap.ac.cn (Y. Gao).

https://doi.org/10.1016/j.net.2019.07.003

$$POF = e^{-\sum_{i=1}^{n_I}\left(\frac{\sigma - S_0}{S_c - S_0}\right)^m \frac{v_i}{v_I}}$$

where v_i is the volume associated with a link; v_I is the total volume of the component; n_I is the link in the weakest link calculation; S_c is the characteristic strength; m is the shape parameter; S_0 is the threshold value.

The procedure for the calculation of the POF is completed in the following steps:

(a) Over the entire component that is being investigated, choose an orthogonal set of coordinates and designate them by the subscripts x, y, and z. The stress components in these directions are then designated σ_x , σ_y, and σ_z for direct stresses, and τ_{xy}, τ_{yz}, and τ_{xz} for shear stresses.
(b) Subdivide the component into integration volumes, represented by points (integration points). This may be achieved by making use of a numerical calculation by the Finite Element Method.
(c) For each integration point, i, calculate the stress components for each loading to which the Graphite Core Component will be subjected. This is typically the output of a three-dimensional finite element calculation of the stresses in the Graphite Core Component.
(d) Calculate the algebraic sum of the values of σ_{xi} at the integration point, which result from the different type of loading, and similarly for the other five stress components.
(e) For each integration point, translate the stress components for the x, y, and z directions into principal stresses σ_1, σ_2, and σ_3.
(f) For each integration point, calculate the equivalent stress resulting from the three principal stresses using the equation in ASME Code sub article HHA-3213 [10]. This is designated σ_{vi}, the point equivalent stress.
(g) The following stress-volume integral is to be completed over the Graphite Core Component:
    (1) Rank the integration volumes in decreasing order of the point equivalent stress (σ_{vi}).
    (2) Moving Threshold Value. To ensure that a sufficient POF calculation volume of material is always used to make multiple links in the weakest link calculation even at very low loads; and allow for likelihood of failure at very low loads. Threshold Value is adjusted depending on $S_{c095\%}$. If the maximum equivalent stress is greater than $S_{c095\%}$, then the current point equivalent stress remains unchanged.

$$s'_0 = s_0$$

If the maximum equivalent stress is less than the value of $S_{c095\%}$, then is recalculated as follows:

$$s'_0 = \frac{\sigma_{max}}{s_{c095\%}} s_0$$

Whereσ_{max} is the highest equivalent stress occurring in the component. Truncate the list of integration points to those where the point equivalent stress is greater than the threshold stress (s'_0).

    (3) For the integration point, calculate and store

$$X_i = \left[\frac{\sigma_{vi} - s'_0}{S_{C095\%} - s'_0}\right]^{m_{095\%}}$$

    (4) Group the integration volumes into groups (designated by the index I, II, III, …), starting with the point of highest stress. The allocation to groups is based on the following two conditions:
    - Condition 1: group volume $V_{\mathrm{I,II,III...}} > V_m$.
    - Condition 2: group stress range as follows:

$$\frac{\max(X_{\mathrm{I,II,III...}}) - \min(X_{\mathrm{I,II,III...}})}{\min.(X_{\mathrm{I,II,III...}})} \geq \Delta$$

Where V_m = a process zone volume, which is calculated from the following equation:

$$V_m = \left[6.369 \times \left(\frac{K_{IC}}{2\sigma_m}\right)^2\right]^3$$

Where K_{IC} = Critical Stress Intensity Factor for mode I, V_m = process zone volume [11] based on fracture toughness and mean tensile strength, σ_m = mean tensile strength.

Δ = the stress range parameter, 20%.

    (5) For each group, compute a probability of survival by summing over the integration volumes within each group as follows:

$$L_\mathrm{I} = \exp\left[-\sum_i X_i \times \frac{V_i}{V_I}\right]$$

L_I is the probability of survival of group I; X_i is defined as in (3); V_i is the volume associated with one sub-element; V_I is the total volume of a group.

    (6) Calculate the probability of survival of the graphite core component by multiplying the probability of survival of the groups.

$$\mathrm{L} = \prod_I L_I$$

L is the probability of survival of the graphite core component.

    (7) Calculate and report the probability of failure:

$$POF = 1 - \mathrm{L}$$

3. Results and discussion

It is known that the highest population density (highest number of failures) is at the average experimental failure load which corresponds to a 50% POF failure load predicted by model. For this reason the 50% POF load is a good basis for comparison with each test case. In order to calculate the predicted failure load, an iterative process is followed. The FEA model is modelled with the 50% POF failure load from experimental results for each test case. The results from the FEA are used to calculate the POF. The difference between the calculated POF and the required 50% POF is used to scale the principal stresses and the POF is recalculated until the predicted POF reaches 50%.

4. Experimental

Two experiments, four point bending and Brazilian disk splitting tests, have been implemented to verify the reliability of the developed assessment method. Fig. 1 shows machine setup for four point bending test. Ten dog-bone samples with each fillet radii were tested. The diagram of a typical specimen with fillet radii, R, is given in Fig. 2. The different fillet radii mean various stress concentration factors of graphite components. The fillet radii, R, in the tests are separately 0 mm, 1 mm, 5 mm, 10 mm. Four point bending test is implemented by MTS Insight Test Frame (E44.204). At least 10 specimens were tested for each case. The Brazilian disk splitting tests were carried out as shown in Fig. 3. Specimens with diameter of 12.7 mm were tested with a loading of 0.5 mm/min 50 specimens have been tested for this experiment.

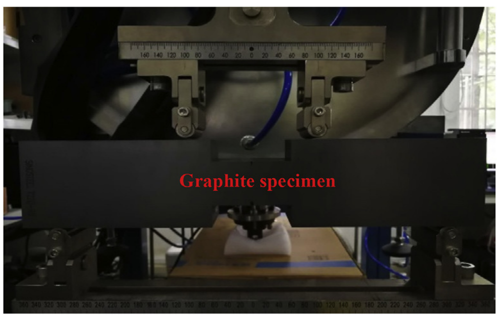

Fig. 1. Machine setup for four points bending tests.

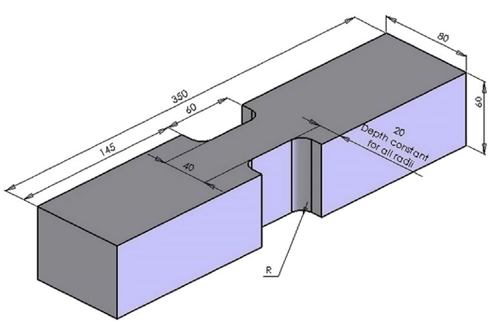

Fig. 2. The diagram of a typical specimen with fillet radii, R.

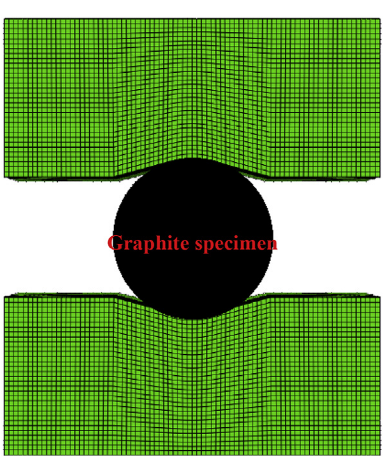

Fig. 3. The diagram of Brazilian disk splitting test.

4.1. Theoretical prediction

4.1.1. Prediction of four points bending of Dog-Bone specimens

A useful failure methodology must provide acceptable failure estimations for the full range of failure probabilities relevant to the particular part. This section compares the failure probability for different load calculated by KTA 3232 and the new method. The specimens were made of super fine grain graphite with the maximum grain size less than 10 μm. The mechanical properties of the graphite are listed in Table 1.

From Fig. 4, it can be seen that the results predicted by new method is more conservative and stress concentration can also significantly influence the failure probability. The Dog-Bone specimens with R = 0 mm obviously show higher failure probability compared with specimens with R = 1 mm, 5 mm, 10 mm at the same displacement, no matter which predicted method was used.

4.1.2. Prediction of four points bending of Brazilian disc splitting tests

The graphite used for Brazilian disc splitting tests was a commercial product graded NBG-18 which was manufactured by SGL, INC. in Germany. The material is a coarse grain graphite with maximum grain size of 1.6 mm.

Fig. 5 shows the curve of POF of Brazilian discs versus loading. The result indicated POF calculated by ASME is very conservative compared with the other methods. The predicted data by the new method is close to the values obtained by KTA3232. The primary reason can be attributed to the weakest link theory introduced in our new method.

4.2. Mesh convergence

The accuracy of the failure assessment depends on the validity of the FE results. And the FE results depend on the refinement of the mesh. Thus a sensitivity of failure probability on FE mesh convergence is undertaken by Brazilian disk splitting tests. And mesh size serves the degree of mesh refinement. These results are presented in Fig. 6. As we can see the predicted POF at same stress didn't show obvious change with the different mesh refinement and failure criteria convergence can be reached at last.

4.3. Verification of failure assessment methodology

4.3.1. Four point bending tests of dog-Bone specimens

Fig. 7 shows comparison between the measured 50% POF failure load and the predicted 50% POF failure loads for Dog-Bone specimens with R = 0 mm. The result shows that KTA 3232 is too acute for failure assessment and the new method is reasonable. Fig. 8 shows that the measured 50% POF failure loads of all Dog-Bone specimens with R = 0 mm, 1 mm, 5 mm, 10 mm are close to predicted 50% POF failure loads by new method. Therefore, the new method is more suitable for the failure assessment of super fine nuclear graphite components.

4.3.2. Brazilian disc splitting tests

Fig. 9 illustrated the predicted 50% POF failure load compared to the measured 50% POF failure load for Brazilian disc splitting tests. The results showed the predicted failure load by ASME is too conservative. The predicted failure loads by KTA 3232 and new method were similar. It can be attributed to no obvious stress concentration symptoms in Brazilian disc. The results also indicated mesh sensibility can be neglected as mesh size (l = 0.3 mm, 0.4 mm, 0.5 mm) has no significant effect on predicted 50% POF failure load.

In summary, the predicted 50% POF failure load by ASME are conservative compared to the measured 50% POF failure load. For

Table 1
Material parameters of super fine grain graphite.

S_c(MPa)	Shape parameter m	Compressive/tensile strength ratio	S_0(MPa)	Modulus(GPa)
33.21	3.74	0.26	24.71	12.7

Table 2
Material parameters of graphite (graded NBG-18).

S_c (MPa)	Shape parameter m	Compressive/tensile strength ratio	S_0 (MPa)	Modulus (GPa)
21.6	5.78	0.264	8.25	11.5

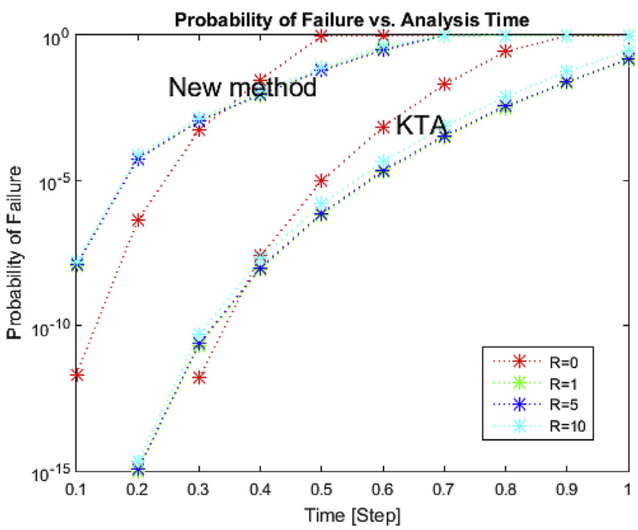

Fig. 4. POF of different Dog-Bone specimens versus load time.

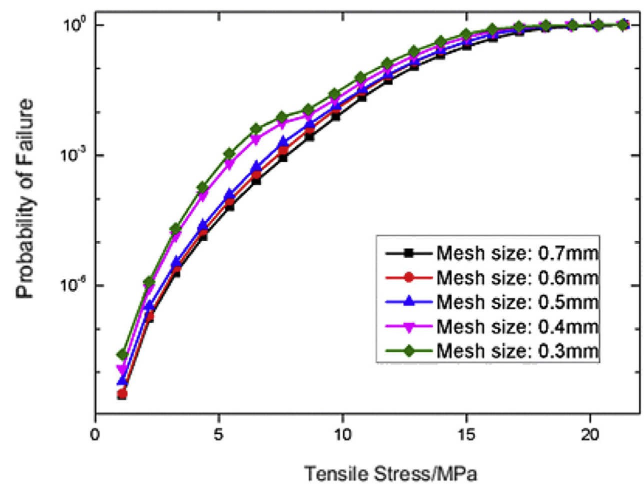

Fig. 6. The effect of mesh size on probability of failure.

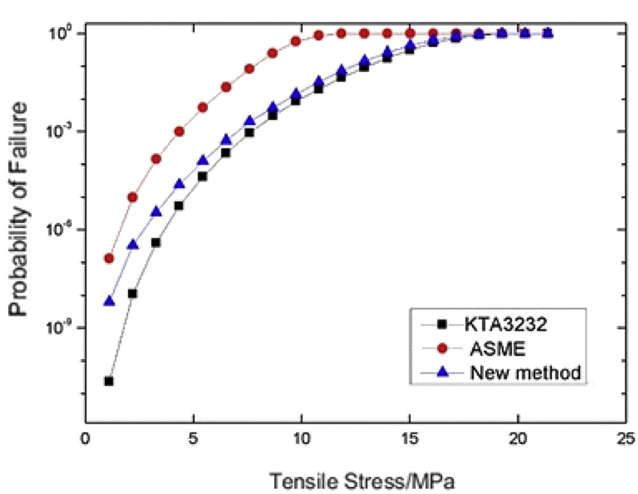

Fig. 5. Failure probability of Brazilian disc specimens at different tensile stress.

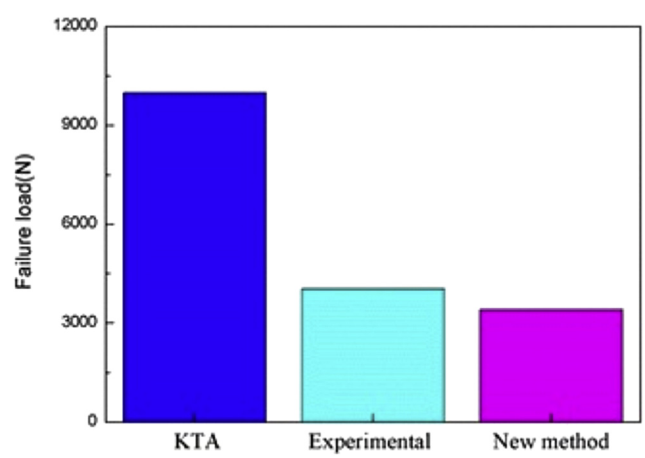

Fig. 7. Comparison between experimental data and predicted results for Dog-Bone specimen with R = 0.

KTA 3232 and new method, the predicted results are closed when no obvious stress concentration occurs. But the predicted data by KTA 3232 could be over aggressive as the KTA method neglects stress concentration effect as referred in Fig. 7.

5. Conclusions

A modified assessment approach based on ASME has been provided in this paper. The new method was compared with probability of failure assessment of nuclear graphite in KTA 3232 and ASME BPVC-III-5. Four point bending tests and Brazilian disc splitting tests were carried out to verify the validation of the new method. The results indicated that:

a. Compared with KTA 3232, the new method can effectively improve the accuracy of POF prediction for super fine grain graphite component as grouping is involved in the estimation.

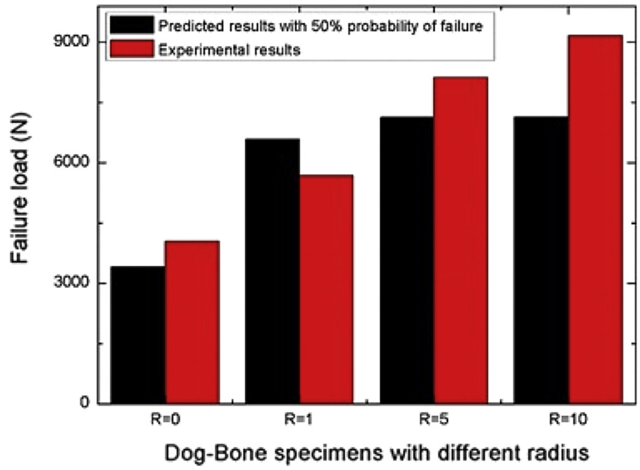

Fig. 8. Comparison between theoretical result by new method and experimental data for Dod-Bone specimens with different radii.

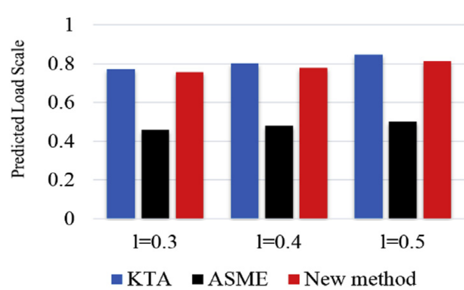

Fig. 9. Prediction for 50% POF failure load scale by different methods (Predicted load scale is the ratio of predicted 50% failure load to measured 50% failure load).

b. The new method is more reasonable as it improves grouping criteria of the existing ASME specification. Also, the method showed little mesh sensitivity in POF predictions. Therefore, the developed approach is more suitable for assessment for super fine grain graphite components.

Meanwhile, the new method retained all advantages which allows for the design of multiple geometries subjected to complex loading conditions. Therefore, geometric optimization of components and failure assessment of graphite components with complex irradiated non-linear material models can also be performed in the new method.

Acknowledgements

The authors greatly acknowledge the financial support from Scientific Instrument and Equipment Development Project CAS Foundation (Grant # YJKYYQ20170061) and National Natural Science Foundation of China (Grant #11802317, 51602336).

References

[1] J. Serp, M. Allibert, O. Benes, et al., The molten salt reactor (MSR) in generation IV: overview and perspectives, Prog. Nucl. Energy 77 (2014) 308–319.
[2] T.H. Becker, T.J. Marrow, R.B. Tait, Damage, crack growth and fracture characteristics of nuclear grade graphite using the Double Torsion technique, J. Nucl. Mater. 414 (2011) 32–43.
[3] T. Becker, Understanding and Modelling Damage and Fracture in Nuclear Grade Graphite, University of Cape Town, 2011.
[4] KTA-3232, Ceramic Components of Reactor Pressure Vessel (Draft), 1992.
[5] R.J. Price, Statistical study of the strength of near-Isotropic graphite, Gen. Atom. Proj. 3224 (1976).
[6] F. Ho, Modified Weibull Theory for the Strength of Granular Brittle Material, General Atomic company, 1979.
[7] J.E. Brocklehurst, M.I. Darby, Concerning the fracture of graphite under different test conditions, Mater. Sci. Eng. 16 (1974) 91–106.
[8] J.P. Strizak, The Effect of Volume on the Tensile Strength of Several Nuclear Grade Graphites, Specific Nuclear Reactors & Associated Plants, 1991.
[9] M.P. Hindley, M.N. Mitchell, C. Erasmus, et al., A numerical stress based approach for predicting failure in NBG-18 nuclear graphite components with verification problems, J. Nucl. Mater. 436 (2013) 175–184.
[10] ASME Boiler and Pressure Vessel Code, SECTION III Rules for Construction of Nuclear Facility Components, HHA-3217 Calculation of Probability of Failure, 2017.
[11] T. Burchell, D.E. III, R. R. Lowden, J. Hunter, C. Hannel, The Fracture Tough of Nuclear Graphite Grades, ORNL/TM-2016/678